PHYSICAL REVIEW C VOLUME 44, NUMBER 6 DECEMBER 1991

Particle multiplicity dependence of high-energy photon production in a heavy-ion reaction

L.G. Sobotka, L. Gallamore, A. Chbihi,* D.G. Sarantites, and D.W. Stracener
Department of Chemistry, Washington University, St. Louis, Missouri 63130

W. Bauer, D.R. Bowman, N. Carlin, R.T. DeSouza, C.K. Gelbke, W.G. Gong, S. Hannuschke, Y.D. Kim, W.G. Lynch, R. Ronningen, M.B. Tsang, and F. Zhu
Department of Physics and The National Superconducting Cyclotron Laboratory, Michigan State University, East Lansing, Michigan 48824

J. R. Beene, M.L. Halbert, and M. Thoennessen†
Oak Ridge National Laboratory, Oak Ridge, Tennessee 37830
(Received 19 July 1991)

The production of high-energy photons in an intermediate energy heavy-ion reaction (65 MeV/nucleon $^{40}Ar + {}^{93}Nb$) is studied by characterizing the events, which produce the photons, by the forward and backward, light and heavy, charged particle production. While the absolute yield of high energy photons increases with increasing charged particle multiplicity, the spectral shape is found to be almost independent of multiplicity. This indicates that the fundamental photon production mechanism is insensitive to the impact parameter but that the production process is more probable for the more violent collisions. This is expected for an incoherent nucleon-nucleon bremstrahlung mechanism but not for a statistical mechanism. This work also provides a comparison of two observables that have been suggested as impact parameter selectors: the high-energy photon yield and the charged particle multiplicity. We find that the photon yield, binned by particle mutiplicity, does not scale as would be expected if both techniques truly measured the impact parameter. This observation can be explained by large fluctuations in the particle multiplicity at fixed impact parameter.

In the last several years considerable theoretical [1–6] and experimental [6–15] effort has been directed toward understanding the production of high-energy photons (those with energies exceeding that of the giant resonance region) in heavy-ion reactions. The production mechanism of these high-energy or hard photons should provide an excellent probe of the dynamics of the reactions, because once created the photons leave the interaction region without rescattering. High-energy photons can be produced by both nucleus-nucleus [2,4] and nucleon-nucleon bremsstrahlung [1,3,5,6]. The former would lead to a strong dependence on the charges of the projectile and target and a quadrupole angular distribution. However, several experiments [7,8,14,15] have shown that the yield does not show the strong charge dependence or the angular distribution expected for nucleus-nucleus bremsstrahlung.

The production of high-energy photons from nucleon-nucleon collisions is dominated by radiation from neutron-proton collisions, as has been discussed by Levinger [16]. Photon emission from nucleon-nucleon collisions will occur throughout the nucleus-nucleus collision. The spectrum of photons will reflect the relative nucleon-nucleon collision velocity distribution. It is useful (and perhaps a bit simplistic) to consider the two extreme pictures. On the one hand, photons will be produced by the initial nucleon-nucleon collisions. On the other hand, after much of the collective translational kinetic energy has been damped, high-energy photon production can be thought of as a statistical process from an equilibrated region of the interaction. The latter process is usually incorporated into statistical model calculations using Levinger's quasideuteron model to deduce the cross section for the inverse process. Such a statistical mechanism implies multiple collisions, and therefore would be isotropic in the moving frame of the emitter. Futhermore, unless the deposited energy is strictly proportional to the number of nucleons that constitutes the statistical emitter, the photon spectrum would exhibit a strong dependence on the extent of energy deposition. This deposited energy would also be reflected in the particle production. Therefore for the statistical process, with the exception noted above, one expects the photon spectrum to be harder for those collisions that produce a larger particle multiplicity.

In the other extreme case, if the first (or first few) neutron-proton collisions are responsible for the hard photon yield [3,5,6], the photon angular distribution would have a slight dipole character in the nucleon-nucleon center-of-mass frame and the shape of the spectrum relatively insensitive to the ultimate energy damping. However, the yield of high-energy photons would be expected to increase as the overlap of the projectile and target increases, simply reflecting more neutron-proton

collisions. Therefore, the dominance of this mechanism would allow the photon yield to be used as an impact parameter selector [1]. The spectral shape, which reflects the distribution of initial relative neutron-proton energies, would be expected to be only weakly dependent on impact parameter. (A weak dependence is expected because the most peripheral collisions will only lead to an overlap of the surface regions where smaller mean nucleon kinetic energies are found.)

The experimental studies mentioned above [7,8,14,15] have shown that the inclusive angular distribution of the high-energy photons is consistent with emission from the nucleon-nucleon center-of-mass frame with the expected angular disribution. This observation provides a strong argument for a dominant leading particle-production mechanism. However, conclusions based on inclusive angular distributions could be misleading in that they contain contributions from collisions at all impact parameters and thus different reaction types. It is possible that the inclusive angular distribution results from the superposition of the contributions of reactions with different admixtures of the leading versus statistical processes.

To remove the uncertainty mentioned above, several studies have been done which have characterized the high-energy photon yield by some particle information [9–13]. Herrmann *et al.* [10] have studied the symmetric system, ^{92}Mo + ^{92}Mo at an energy of 19.5 MeV/nucleon. In this experiment photon spectra were obtained in coincidence with binary reactions characterized by the total kinetic-energy loss. The spectra become significantly harder with increasing total kinetic-energy loss, thus providing evidence that a statistical mechanism is relevant in this reaction. Recent [6] reanalysis of these same data indicate that leading particle interactions dominate the high-energy photon production, but that statistical emission does make a significant contribution to the photon production at the highest-energy losses. Hingmann *et al.* [9] report on a study of a higher-energy reaction, 44 MeV/nucleon ^{44}Ar + ^{158}Gd, for which the events are characterized as central, peripheral, or grazing by conditions placed on the fragments detected in a forward heavy-ion detector. The absolute yield of the high-energy photons increases with centrality and the spectral shape exhibits only minor changes with centrality (the spectra become slightly harder for the more central collisions). Similar results have also been reported in the study [12] of 85 MeV/nucleon ^{36}Ar + ^{27}Al. In this experiment the events were characterized by the forward charged particle multiplicity.

The present work is a study similar to the last one mentioned above except done with a more massive system and with a more complete event characterization. The system studied is 65 MeV/nucleon ^{40}Ar + ^{93}Nb. The events are characterized by the forward and backward, light- and heavy-ion multiplicities. The rather complete charged-particle production information allows us to address the question of whether both high-energy photon production and particle multiplicity are measures of impact parameter.

The experiment was performed at the K1200 cyclotron of the National Superconducting Cyclotron Laboratory at Michigan State University. The beam of 65 MeV/nucleon ^{40}Ar had an average intensity of 0.07 particle nanoamperes. This intensity was limited by counting-rate considerations for the charged-particle detection device, the Dwarf Ball and Wall [17], which consists of 104 fast plastic-CsI(Tl) scintillator phoswich detectors, each capable of light-ion identification ($p, d, t, ^3$He, and α particle) and element identification for $Z < 15$. The solid angle coverage of the Dwarf system was 85% of 4π.

In order to suppress secondary electrons, each detector was covered by an absorber foil. These foils varied from 4.0 mg/cm^2 of Ta, for the most backward detectors, to 6.3 mg/cm^2 of Ta, for the detectors at 14.8°. The most forward detectors (centered at 8.1°) were covered by a thick Pb sheet (254 mg/cm^2). As a result of these absorbers and the varied thickness of the fast plastic layer the low-energy detection threshold is a function of angle (see Ref. [17]). Futhermore, due to rather modest depth of the CsI scintillators (varying from 4 mm at backward angles to 20 mm for the Wall elements) a substantial fraction of the light ions punched through. Nevertheless, even for these cases we are still able to distinguish the light ions from the heavy ions. Therefore, for the purpose of this analysis, the charged particles are characterized by whether they are light ($Z < 3$) or heavy ($Z \geq 3$) and by the emission angle. As we have done before, the angular region is coarsely, and rather arbitrarily, divided into that spanned by the forward Wall ($\theta_{\rm lab} < 35^\circ$) and the more backward angles covered by the Ball.

The photons were detected in two BaF_2 arrays, each consisting of 19 close-packed detectors. The individual BaF_2 detectors have hexagonal cross sections of 36.6 cm^2 and are 20 cm long. The two arrays were positioned, one on top of the other, 50 cm from the target, at 90° to the beam. The detectors were individually calibrated with sources (extending up to 2.62 MeV) and the cosmic-ray peak, the data for which were acquired during a 133 minute beam-off run. The most probable energy deposition for a cosmic ray was calculated with the simulation code GEANT [20]. The results of GEANT have been verified to give the correct cosmic-ray energy deposition in a separate experiment where the BaF_2 detectors were calibrated using the 15.1 MeV photon produced in the reaction ^{12}C(p,p'). Neutron pulses were distinguished by pulse shape discrimination [6]. (The time-of-flight information was also used to reject neutron pulses, but this technique was only effective for pulses corresponding to deposited energies of less than 15 MeV, which are not of interest for the present study.) Each array of 19 BaF_2 detectors was treated as one detector after energy calibration and neutron rejection. (If any of the 19 individual detectors recorded a neutron pulse the sum information from the entire pack was rejected.) Each pack subtended 2.1% of 4π. Cosmic-ray pulses proved to be negligible, primarily due to the coincidence resolving time.

The charged-particle multiplicity distributions are shown in Fig. 1(a). This figure shows how the total multiplicity (thickest line) is composed of light ions (thin lines) and heavy ions (lines of intermediate thickness), emitted to forward and backward angles. The overwhelming majority of the multiplicity is due to the light ions, with the

contribution from angles larger than 35° exceeding that measured forward of this angle. On the other hand, the much smaller heavy-ion contribution is forward focused. Coincidence summing, primarily in the most forward detectors, reduces these measured multiplicities. This effect is small except for the largest multiplicities, where it distorts the distribution. The photon-energy spectra acquired in coincidence with various multiplicity bins of light and heavy, forward and backward charged particles are shown in Figs. 1(b)–1(f). The most striking feature of these spectra is that the spectral shape is very nearly the same for all the gating conditions. Beyond this, we observe that in all cases, the larger the particle multiplicity, the larger the differential photon multiplicity. However, while the above is true, the magnitude of the increase varies considerably depending on the particle selection condition. For both light and heavy ions, a large charged-particle multiplicity selection for the more backward angles (Ball) is far more effective at increasing the probability of high-energy photon production then a similar selection on forward multiplicity (Wall). This is most clearly seen in the case of light ions [compare Figs. 1(c) and 1(d)]. In our previous work we have shown that large backward multiplicity is the best single indicator of linear momentum transfer [18,19]. Therefore this figure illustrates that large momentum transfer events not only copiously produce fragments but also produce the most high-energy photons.

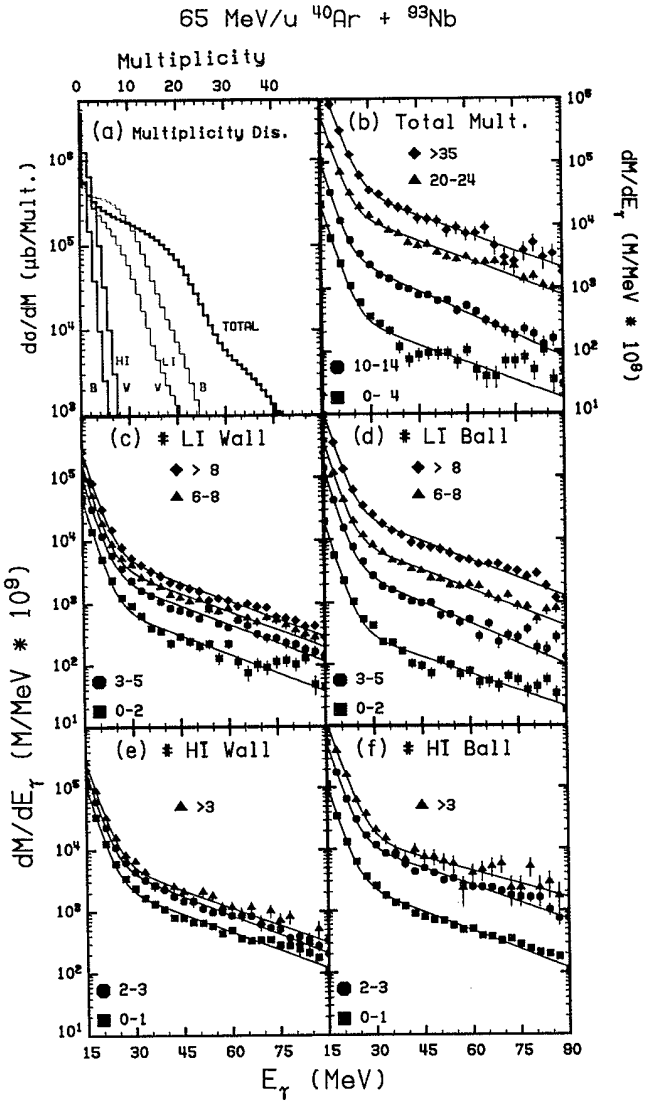

FIG. 1. (a) Total charged particle multiplicity (thickest line) and its composition in terms light ions (thin lines) and heavy ions (intermediate thickness lines) for the Wall (W) and the Ball (B). The Wall subtends angles between approximately 5° and 35°, while the Ball subtends the backward angles to approximately 170°. The photon spectra gated on selected bins of (b) total charged particle multiplicity, (c) forward light-ion multiplicity, (d) backward light-ion multiplicity, (e) forward heavy-ion multiplicity, and (f) backward heavy-ion multiplicity. The charged particle multiplicity bins are indicated in the figure. The ordinate is differential multiplicity (mult./MeV), calculated assuming isotropic emission.

In order to get the actual photon-energy distribution and the correct absolute photon mutiplicity, we have unfolded the photon spectra. The response of the individual BaF_2 packs was simulated with GEANT for photons generated 55 cm from the front face. (The difference between 55 cm and the actual distance of 50 cm is insignificant.) The experimental spectra were fitted by sums of exponential functions [lines in Figs. 1(b)–1(f)] and the fits where unfolded. A sample of this procedure is shown in Fig. 2. The fit (thin line) represents the raw data quite well. The unfolding procedure (the result of which is indicated by the thick line in Fig. 2) increases the absolute multiplicity, in this high energy region, as well as making the spectrum slightly harder.

Unfolded spectra are shown as solid symbols in Fig. 3 for gates on the total multiplicity. (As these spectra result from the unfolding of fits to the raw data, no error bars are assigned to the individual points. A reasonable estimate for the uncertainty of the unfolded spectrum would be given by a region enveloped by symbols approx-

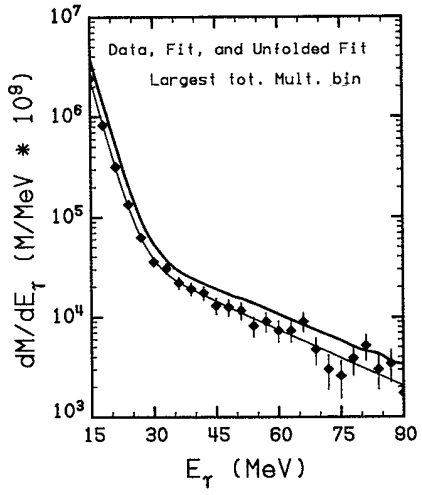

FIG. 2. Shown are the data (diamonds), fit of the data (thin line), and the spectrum resulting from the unfolding of the fit (thick line) for events with a total charged particle multiplicity greater than 35.

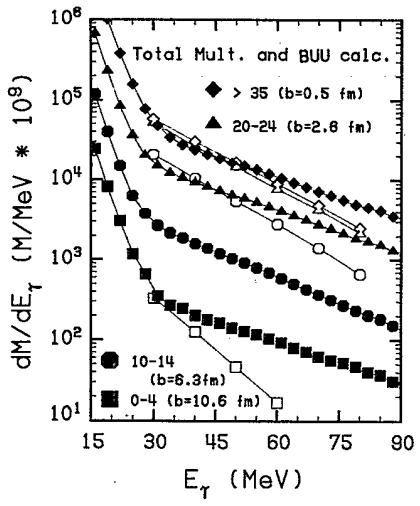

FIG. 3. Unfolded spectra are shown as solid symbols for four bins on the total charged particle multiplicity. BUU calculations at the corresponding impact parameters are shown as open symbols.

imately $\frac{1}{2}$ the size of those in the figure at the low-energy end to twice the size of the symbols at the high-energy end.) The photon yield in the high-energy region ($E_\gamma >$ 30 MeV) is well described by a single exponential with an inverse slope parameter of E_0(data) = 23.9±3.7 and 25.3±2.4 MeV for the data gated on the total multiplicity (Figs. 3) and the data gated on backward light-ion multiplicity (not shown) , respectively. In both of these cases, the inverse slope parameter exhibits no statistically significant trend with particle multiplicity. The previous work on the substantially lighter system ^{36}Ar + ^{27}Al at 85 MeV/nucleon observed a 40% increase in the inverse slope paramenter for central collisions as compared to the most peripheral [12]. Our particle-multiplicity-sorted data are inconsistent with such a large change.

The similarity of the photon-energy distribution for the different gates on multiplicity suggests that the fundamental neutron-proton bremsstrahlung spectrum is similar for all events and simply that the number of neutron-proton collisions increases with violence, as measured by the particle multiplicity. As mentioned previously, this is the trademark of a leading particle collision production mechanism. In such a picture, the spectrum is mainly determined by the initial relative nucleon-nucleon velocity distribution, which is only weakly dependent on geometry, while the probablity is proportional to the collision frequency, which is primarily determined by geometry.

High-energy photon production by leading and near leading particle-particle interactions can be simulated within the framework of the Boltzmann-Uehling-Uhlenbeck (BUU) equation [6]. This treatment describes the time development of the system by a transport equation for the one-body density matrix, derived from the Bogoliubov, Born, Green, Kirkwood, Yvon (BBGKY) hierarchy. However, in order to compare our data to BUU simulations we must convert the experimental particle multiplicity scale to an impact parameter scale. We assume that the charged-particle multiplicity increases monotonically with decreasing impact parameter. One must keep in mind that the relationship need not be so simple (in which case the comparison to theory would be invalid.) To unfold the multiplicity distribution, we assumed that the interaction radius, below which reactions start and the detection device is sensitive, was $R_{\rm int}$ = 11.75 fm, consistent with the systematics used in Ref. [21]. The calculations for the impact parameters corresponding to the mean multiplicity of the multiplicity bins are included in Fig. 3 as open symbols. The overall yield of the high-energy photons, which is determined by the most central collisions, is well reproduced. However, the calculations underestimate the inverse slope parameter [E_o(BUU) = 15.5 ± 0.5 MeV for all impact parameters except the largest] and fail to reproduce the regular decrease in the photon yield with decreasing particle multiplicity.

The underprediction of the inverse slope parameter suggests that either the extreme components of the momentum distributions of the colliding nuclei are underestimated or that the elementary photon production cross sections for large relative nucleon energies is underestimated. The second discrepancy, that the decrease of the photon yield with impact parameter (calculations) does not reproduce the observed trend with particle multiplicity, is illustrated in Fig. 4 where the integrated photon multiplicity is plotted versus impact parameter (a deduced parameter in the case of the data). The calculated yield follows the overlap volume of the colliding partners (solid line) while the data exhibit an exponential decline with the deduced impact parameter. If one believes in the leading particle production mechansim, and thus the overriding role played by the geometry of the collision, one is led to suspect that the difference mentioned above must be ascribed to an inability to simply relate impact parameter to particle multiplicity. It is reasonable to expect that there exists a broad particle

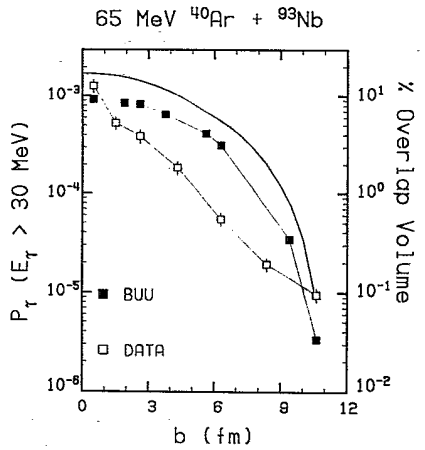

FIG. 4. Integrated yield of photons with energy exceeding 30 MeV. The data are shown as open symbols and are plotted as a function of a deduced impact parameter. The BUU reaction symulations are shown as solid symbols. The solid line is the percent overlap of two spheres averaged over straight line trajectories.

multiplicity distribution (reflecting a broad thermalized energy distribution) for a fixed impact parameter. In this case, one can only expect a comparison between a calculation (at fixed impact parameter) and experimental data (at fixed multiplicity) to be valid on the average, if the quantity being studied is not correlated directly to the particle production mechanism. If there were a direct correlation between high-energy photon production and charged-particle production, then the high-energy photon production would track the charged particle multiplicity in a fashion which might not be given by a calculation which ignores the fluctuations and relates an average particle multiplicity to an average impact parameter. This is what is suggested by the comparison of data and calculations shown in Figs. 3 and 4. At lower energies, deeply inelastic collisions provide an example of such a correlation. The impact parameter does not uniquely determine the energy loss, but given an energy loss the number of evaporated particles and the hardness of the statistical photon spectrum will track one another. In the energy domain of the present work, where statistical photon emission does not appear to play a significant role, a plausible physical argument for such a correlation also exists, as long as the photon energy is small compared to the total thermalized energy. The violent nucleon-nucleon collisions which produce high-energy photons are efficient at mixing the momentum components, decreasing the momentum components along the beam direction and generating transverse components. Therefore violent leading neutron-proton scattering fosters the development of phase-space distributions that appear thermal, thus increasing the multiplicity of particles that will be evaporated at a later stage of the reaction. Needless to say, if the photon energy is a significant part of the total thermalized energy, energy conservation will require an anticorrelation between photon and particle production. As a final comment, the presence of strong-particle multiplicity fluctuations at fixed impact parameter would also explain why photon spectra gated on different multiplicity regions have indistinguishable inverse slope parameters.

In summary, we have made a detailed study of the charged-particle multiplicity dependence of high-energy photon production in the reaction 65 MeV/nucleon ^{40}Ar + ^{93}Nb. While the photon yield does increase dramatically with charged-particle multiplicity, the shape of the spectrum remains essentially constant. This observation provides support for the interpretation that the high-energy photon production in intermediate-energy collisions results from nucleon-nucleon collisions early in the nucleus-nucleus collision dynamics. Calculations based on the Boltzmann-Uehling-Uhlenbeck equation for the time development of the one-body phase-space distribution and photon production via incoherent nucleon-nucleon collisions reproduce the overall photon yield but underestimate the slope and fail to reproduce the trend of the differential photon multiplicity with charged-particle multiplicity. The first difference is likely a failure of the calculation and suggests that more attention must be paid to the tails of the momentum distributions. The second difference indicates that impact parameters deduced by unfolding the particle multiplicity distribution are inconsistent with those deduced from the magnitude of the high-energy photon yield. This inconsistency may result from large fluctuations in the particle multiplicity at fixed impact parameter.

This work was supported by the Director, Office of Energy Research, Office of High Energy and Nuclear Physics, Nuclear Physics Division of the U. S. Department of Energy, under Contract Nos. DE-FG02-87ER40316 and DE-FG02-88ER40406. Oak Ridge National Laboratory is operated by Martin Marietta Energy Systems, Inc. under Contract No. DE-AC05-84OR21400 with the U.S. Department of Energy. Additional support was provided by the National Science Foundation under Grants Nos. PHY-86-11210, PHY-89-13815, and PHY-90-17077.

---

* Present address: Grand Accelerateur National d'ions Lourds, GANIL 14021 Caen Cedex, France.

† Present address: National Superconducting Cyclotron Laboratory, Michigan State University, East Lasing, MI 48824.

[1] N. Nifenecker and J.P. Bondorf, Nucl. Phys. **A442**, 478 (1985).

[2] D. Vasak, B. Muller, and W. Greiner, J. Phys. G **11**, 1309 (1985); D. Vasak, Phys. Lett. B **176**, 276 (1986).

[3] W. Bauer, W. Cassing, U. Mosel, and M. Tohyama, Nucl. Phys. **A456**, 159 (1986); W. Bauer, G.F. Bertsch, W. Cassing, and U. Mosel, Phys. Rev. C **34**, 2127 (1986).

[4] K. Nakayama and G.F. Bertsch, Phys. Rev. C **36**, 1848 (1987).

[5] J. Randrup and R. Vandenbosch, Nucl. Phys. **A490**, 418 (1989).

[6] W. Cassing, V. Metag, U. Mosel, and K. Niita, Phys. Rep. **188**, 365 (1990).

[7] K.B. Beard *et al.*, Phys. Rev. C **32**, 1111 (1985).

[8] J. Stevenson *et al.*, Phys. Rev. Lett. **57**, 555 (1986).

[9] R. Hingmann *et al.*, Phys. Rev. Lett. **58**, 759 (1987).

[10] N. Herrmann *et al.*, Phys. Rev. Lett. **60**, 1630 (1988).

[11] V. Metag, Nucl. Phys. **A488**, 483c (1988).

[12] M.K. Njock *et al.*, Nucl. Phys. **A488**, 503c (1988).

[13] A. Lampis *et al.*, Phys. Rev. C **38**, 1961 (1988).

[14] R.J. Vojtech *et al.*, Phys. Rev. C **40**, R2441 (1989).

[15] C.A. Gossett *et al.*, Phys. Rev. C **42**, R1800 (1990).

[16] J.S. Levinger, Phys. Lett. **82B**, 181 (1979); J.S. Levinger, *Nuclear Photo-Disintegration* (Oxford Univ. Press, Oxford, England, 1960).

[17] D.W. Stracener *et al.*, Nucl. Instrum. Methods **A294**, 485 (1990).

[18] T.B. Tsang *et al.*, Phys. Lett. B **220**, 492 (1989).

[19] A. Chbihi *et al.*, Phys. Rev. C **43**, 652 (1991).

[20] R. Brun *et al.*, GEANT3 *Users Guide* (Data Handling Division DD/EE/84-1, CERN, 1986).

[21] W.W. Wilcke *et al.*, At. Data Nucl. Data Tables **25**, 389 (1980).